Journal of Theoretical and Applied Information Technology
20th June 2014. Vol. 64 No.2

ISSN: 1992-8645 www.jatit.org E-ISSN: 1817-3195

APPLICATION OF SPECTRUM EXPRESSION AND INDEPENDENT COMPONENT ANALYSIS IN COMPOSITION ANALYSIS OF MIXED PIGMENT

[1]GONGMING WANG, [2]ZHIYONH LIU
[1] Department of Information Art and Design, Academy of Art and Design, Tsinghua University, Beijing, China
[2] Institute of Computing Technology, Chinese Academy of Sciences, Beijing, China
E-mail: [1] gongmingwang@126.com, [2] zyliu@ict.ac.cn

ABSTRACT

Reflectance spectroscopy (RS) is suitable for the composition analysis of mixed pigment, because the corresponding basic pigment can be determined by calculating the spectrum similarity. However, the spectrum similarity between known pigment and mixed pigment may be not the one between known pigment and the most similar basic pigment, and the known pigment with the largest spectrum similarity may be not the highest proportion of mixed pigment, due to the possible relationship among the basic pigments. Thus, it is easy to affect the accuracy of composition analysis. In this study, a composition analysis method of mixed pigment based on spectrum expression and independent component analysis (ICA) is proposed. First of all, the spectral information of mixed pigment is obtained with spectrometer, and is expressed as the mixed signal. After that, the independent signal (spectrum of basic pigment) is generated with ICA. Then, the type of basic pigment is determined by calculating the spectrum similarity between basic pigment and known pigment. Finally, the percentage of basic pigments is obtained by solving Kubelka-Munk equation system. To validate this method, the 4, 5, 6 simulated spectrums were mixed from four spectrums of Munsell color card, and the experiments were carried out in two aspects. On the one hand, the composition analysis of three groups of original simulated spectrums was executed. On the other hand, each group was mixed with one disturbance spectrum in order to test the anti-interference performance of this method. The separated K/S curve is very similar to the original K/S curve. The average similarity is 96.29%, and the maximum one can reach to 98.37%. The calculated percentage of basic pigment closes to the original one. It can be seen that this method is suitable for composition analysis of mixed pigment.

Keywords: *Color, Composition Analysis, Spectrum, Similarity, Independent Component Analysis, Munsell*

1. INTRODUCTION

The composition analysis of mixed pigment can determine the type and percentage of basic pigment that constitutes the mixed pigment, which is widely used for criminal identification [1], cultural relic identification [2], synthetic dye [3] and other fields. Reflectance spectroscopy (RS) [4] is suitable for composition analysis of mixed pigment. First, the type of basic pigment is determined by comparing the spectrum similarities between known pigments and mixed pigments [5]. Second, the percentage is calculated by solving Kubelka-Munk equation system. This method is simple and efficient, and has a certain application value. However, the spectrum similarity between known pigment and mixed pigment may be not the one between known pigment and the most similar basic pigment, and the known pigment with the largest spectrum similarity may be not the highest proportion of mixed pigment, due to the possible relationship among the basic pigments. Thus, it is easy to affect the accuracy of composition analysis. In addition, the experimental result is only effective for several kinds of pigments [6], does not have universal applicability.

It can be seen that the accuracy of type judgment of basic pigment is the main factor that affects the accuracy of RS. According to the Kubelka-Munk theory, the spectrum of mixed pigment is the linear combination of spectrums of basic pigments. Thus, the calculated spectrum similarity is the synthesis of spectrum similarities between known pigment and all basic pigments, not the one between known pigment and a basic pigment. In this case, even if the known pigment is one of the basic pigments, the

ISSN: 1992-8645 www.jatit.org E-ISSN: 1817-3195

calculated spectrum similarity doesn't reach to 1. In addition, the dimension of spectral curve is often hundreds of thousands, and has the problem of "dimension disaster"[7]. In essence, all known pigments have no homologous with the mixed pigment. Thus, the difference of all spectrum similarities is a little [8], and it isn't convenient to determine the type of basic pigment accurately. The above disadvantages in similarity calculation are the root cause of the inaccuracy of type of basic pigment.

The process of mixing basic pigments can be regarded as the linear combination of random signals by taking spectrum as random signal. Independent component analysis (ICA) [9] is an effective tool for separation of linear mixed signal, and the independent signal can be deduced from the mixed signal. In this study, a composition analysis method of mixed pigment based on spectrum expression and ICA is proposed. First, the color of mixed pigment is expressed as reflection spectrum, in order to solve the "metamerism" problem. Second, spectrum vector is regarded as the mixed signal, and the independent signal can be deduced with ICA. Third, the independent signal is taken as the spectrum of basic pigment, and the type of basic pigment is determined by comparing the spectrum similarities between basic pigments and known pigments. Finally, the percentage of basic pigment is obtained by solving Kubelka-Munk equation system. To validate this method, the simulated spectrum was generated from Munsell color system, and the experiments of composition analysis of mixed pigment were carried out under the circumstance of normality and disturbance. The experiment results show that this method can accurately get the type and percentage of basic pigment, and is suitable for the composition analysis of mixed pigment.

The remainder of the paper is organized as follows: the advantage of spectrum expression, Kubelka-Munk theory and ICA are introduced in Section 2; the proposed composition analysis method of mixed pigment is described in Section 3; the composition analysis experiments are carried out in Section 4; and the conclusion and future work are shown in Section 5.

2. RELATED WORKS

2.1 Spectrum Expression of Mixed Pigment

Spectrum is the essential factor to determine surface color of object, and it has no difference along with the change of environment and observer. Thus, it can ensure the accuracy of color quantization and analysis. The Kubelka-Munk theory is useful for the composition analysis of mixed pigment, because it reveals the relationship between mixed pigment spectrum and basic pigment spectrum.

2.1.1 Spectrum expression of pigment

The tristimulus values representation is widely used for color representation in color engineering. Its theoretical basis is the three-dimensional (3D) color theory by Grassmann who is the founder of linear algebra in 1853[10]. That is to say, three variables are sufficient to define any color. Its physiological basis is the perception-response difference between three cones of human eye to color component [11]. The variable (X,Y,Z) is used to describe color [12]. And the component X, Y and Z are used to describe the perception intensities of three cones. The calculate method is shown in equation 1.

$$\begin{bmatrix} X \\ Y \\ Z \end{bmatrix} = k\int_{\lambda_{min}}^{\lambda_{max}} S_D(\lambda)\cdot\rho(\lambda)\cdot\begin{bmatrix} \bar{x}(\lambda) \\ \bar{y}(\lambda) \\ \bar{z}(\lambda) \end{bmatrix} d\lambda \qquad (1)$$

where λ_{min} and λ_{max} are the minimum and maximum spectrums of visible light, $S_D(\lambda)$ is the spectral power distribution of light source, $\rho(\lambda)$ is the spectral reflectance, $\bar{x}(\lambda)$, $\bar{y}(\lambda)$ and $\bar{z}(\lambda)$ are the standard colorimetric tristimulus values from observer with normal color recognition. According to the tristimulus values theory, all kinds of 3D color representations are proposed, such as XYZ, LAB, CMY and RGB.

The "metamerism" problem exists in the tristimulus values representation. That is to say, the tristimulus values of two different colors may be equal after integrated by equation 1. Thus, they may be seen as the same color. And the accuracy of copy and analysis of artwork would be affected by color aberration from this phenomenon. Generally speaking, the root reason is that the integral operation result in formula 1 masks the spectral reflectance difference between different colors. In addition, because the resolution of cones is limited, only seven colors in the different intervals of visible light can be distinguished. Therefore, the accuracies of $\bar{x}(\lambda)$, $\bar{y}(\lambda)$ and $\bar{z}(\lambda)$ in formula 1 are affected.

It is reported that the surface color of object is determined by reflection spectrum on the surface of object. The reflection spectrum is the inherent physical property and independent on the environment and observer [13]. Thus, it can describe the color characteristics of the pigment

Journal of Theoretical and Applied Information Technology
20th June 2014. Vol. 64 No.2

ISSN: 1992-8645 www.jatit.org E-ISSN: 1817-3195

itself, and avoid the uncertainty of type judgment of pigment derived from "metamerism" problem.

From the formula 1, it can be seen that the type judgment of pigment is mainly determined by the following three factors: pigment, environment and observer. The change of any factors would influence the result of tristimulus value representation [14], which affects the accuracy of color quantization and analysis. However, spectrum expression does not have this problem.

To sum up the above statements, the accuracy of color representation is the premise of composition analysis of mixed pigment, and the accuracy of spectrum expression is better than the one of tristimulus values representation. Thus, spectrum expression is suitable for the composition analysis of mixed pigment.

2.1.2 Kubelka-Munk theory

When light shines on the surface of opaque medium, besides a few is reflected, most of light enters into the medium, and the color is generated by absorption and scattering. The relationship between spectral reflectance and absorption/scattering is deduced by Kubelka and Munk [15].

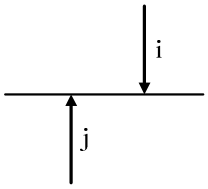

Figure 1: Incident and reflected light in any position

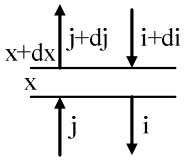

Figure 2: Light reflection effect from infinite lamella

Vertical downward is the positive direction, and incident light is along with vertical direction. The bottom of medium is the origin of coordinates $x=0$, and the value of x is gradually increasing from bottom to top. In figure 1, the incident and reflected light in any place are i and j. The incident light i include the original incident light, the reflected light of pigment particles on medium interface, and the incident light reflected on external surface. Similarly, the reflected light j include the reflected light of pigment particles on medium interface, and the reflected light on bottom layer. The medium with thickness of D is divided into a series of successive infinite lamellas. Absorption, reflection and transmission would be taken place when i and j go through any infinite lamella. In figure 2, the thickness, absorption coefficient and scattering coefficient of any lamella are dx, K and S. The variation of i and j is as follows.

$$\begin{cases} dj = -Kjdx - Sjdx + Sidx \\ -di = -Kidx - Sidx + Sjdx \end{cases} \quad (2)$$

where dj include scattering $Sidx$ of i, scattering $-Sjdx$ of j and absorption $-Kjdx$ of medium to j. The reason of negative sign in $-Sjdx$ and $-Kjdx$ is that the positive direction of x is vertical downward. The interpretation of di is similar. The solving process of this equation is as follows.

The formula 2 can be written

$$\frac{dj}{dx} = S\cdot(i - aj) \quad \frac{di}{dx} = S\cdot(ai - j) \quad (3)$$

where $a = 1 + K/S$. Using derivative formula of quotient of two functions, it concludes

$$\frac{d(j/i)}{dx} = S\cdot\left(\frac{j^2}{i^2} - 2a\frac{j}{i} + 1\right) \quad (4)$$

Let spectral reflectance of medium with thickness of x is $r = j/i$, we have

$$\frac{dr}{dx} = S(r^2 - 2ar + 1) \quad (5)$$

Using integration, this is

$$\int \frac{dr}{r^2 - 2ar + 1} = S\int dx \quad (6)$$

Let spectral reflectance of mediums with thickness of 0 and D are R_g and R. The formula 6 can be written

$$\int_{R_g}^{R} \frac{dr}{r^2 - 2ar + 1} = \frac{1}{2b} ln \frac{(R - a - b)(R_g - a + b)}{(R - a + b)(R_g - a - b)}$$
$$= S\int_0^D dx = SD \quad (7)$$

where $b = \sqrt{a^2 - 1}$. It concludes

$$R = \frac{1 - R_g(a - b\,coth(bSD))}{a + b\,coth(bSD) - R_g} \quad (8)$$

where $coth(bSD)$ is the coth of bSD. When $D \to \infty$, the formula 8 can be simplified

$$R = 1 + K/S - \left[(K/S)^2 + 2(K/S)\right]^{1/2} \quad (9)$$

It concludes

$$K/S = \frac{(1 - R)^2}{2R} \quad (10)$$

The formula 10 is named as the simplified Kubelka-Munk formula. The absorption/scattering

ISSN: 1992-8645 www.jatit.org E-ISSN: 1817-3195

ratio of mixed pigment can be regarded as the linear combination of the ones of all basic pigments. That is

$$(K/S)_{mix} = (K/S)_w + c_1(K/S)_1 + \ldots + c_n(K/S)_n \quad (11)$$

where $(K/S)_{mix}$ and $(K/S)_w$ are the absorption/scattering ratio of mixed pigment and substrate, $(K/S)_i$ and c_i are absorption/scattering ratio and percentage of i-th pigment, $i = 1,2,\cdots,n$.

2.2. Independent Component Analysis

2.2.1 Blind source separation

When the parameters of source and transmission channel are unknown, blind source separation (BSS) [16] can restore the independent component from observed signal, according to the statistical characteristic of input source signal. It is widely used in speech enhancement [17], communication system [18], biological medicine [19], seismic survey [20], information security [21] and other fields. Especially, the successful application in wireless communication and biological medicine has promoted its rapid development.

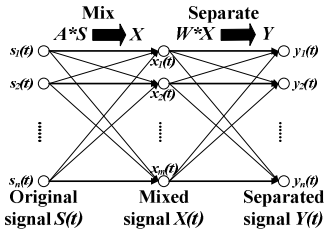

Figure 3: Basic mathematical model of BSS

The basic mathematical model of BSS is shown in figure 3. m mixed signals (or are called observed signals) $x_j(t)$ are generated from n independent original signals $s_i(t)$, $i = 1,2,\ldots,n$, $j = 1,2,\ldots,m$.

$$x_j(t) = \sum_{i=1}^{n} a_{ji} s_i(t) \quad (12)$$

where a_{ji} is the mixing coefficient. Let original signal vector is $S(t) = [s_1(t), s_2(t), \cdots, s_n(t)]^T$, observed signal vector is $X(t) = [x_1(t), x_2(t), \cdots, x_m(t)]^T$, mixing matrix is $A = \lfloor a_{ji} \rfloor_{m \times n}$. Then, the formula 12 can be written

$$X(t) = A \cdot S(t) \quad (13)$$

The result of BSS is a $n \times m$ separative matrix W. The multiplication $Y(t)$ of W and $X(t)$ should be close to $S(t)$

$$Y(t) = W \cdot X(t) \quad (14)$$

Not all the mixed signals can be separated using BSS, the separable observed signals must meet the following conditions.

(1) The number of observed signals isn't less than the one of original signals, e.g. $m \geq n$.

(2) The mixing matrix A is full rank.

All components $s_i(t)$ of original signal $S(t)$ are independent each other, and only up to one component obeys gaussian distribution.

If the above requirements are satisfied, $Y(t)$ would be an estimation of $S(t)$.

In practice, BSS algorithm have two uncertainty: order uncertainty and amplitude uncertainty. The former refers that the order of separated signal is different from the one of original signal. The later refers that the amplitude of separated signal is different from the one of original signal. However, the independent characteristic of signal couldn't be affected, because the information of signal is determined by waveform. Therefore, the above requirements are still met, and the effect of BSS algorithm is all the same[22].

2.2.2. FastICA algorithm

BSS algorithms are divided into three kinds: BSS algorithm based on ICA, BSS algorithm based on second order statistics and BSS algorithm based on sparsity of original signal. Among these methods, BSS algorithm based on ICA (denoted as ICA for convenience) is widely used. There are a variety of ICA algorithms, such as ICA algorithm based on maximum likelihood criterion, ICA algorithm based on minimum mutual information, ICA algorithm based on information maximization and fast fixed-point ICA algorithm (FastICA). Among them, FastICA is applied widely[21], because it has the characteristics of iterative stability, fast convergence and separative matrix orthogonality.

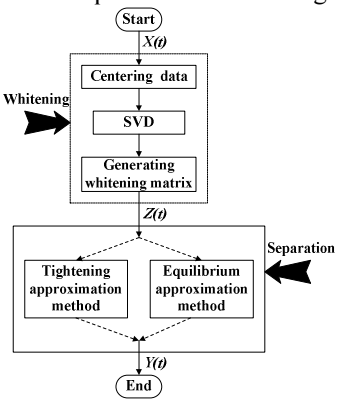

Figure 4: Implementation process of FastICA algorithm

The implementation process of FastICA mainly includes two phases: whitening and separation, which is shown in figure 4. The operation sequence of whitening is: centering data -> singular value decomposition (SVD) -> generating whitening matrix. In this phase, the observed signal $X(t)$ is

Journal of Theoretical and Applied Information Technology
20th June 2014. Vol. 64 No.2

ISSN: 1992-8645 www.jatit.org E-ISSN: 1817-3195

converted into the orthonormal signal $Z(t)$, in order to ensure the independence of signal. The main operation in the phase of separation is constructing the separative matrix. The main strategies include tightening approximation method and equilibrium approximation method. The former is also called one-dimension algorithm, and only one independent component is choosen and updated at a time. The later is also called multi-dimension algorithm, and all independent components are updated at the same time.

2.2.3. Composition analysis of mixed pigment

Spectrum is the accurate expression of pigment, and the spectrum of mixed pigment is the linear combination of spectrums of basic pigments. First, the spectrum is taken as the random signal. Second, based on the spectrum database of known pigments, the type and percentage of basic pigment are calculated by integrating with ICA, spectrum similarity, Kubelka-Munk theory, etc. Finally, the traceability of mixed pigment is achieved.

3. METHODOLOGY

3.1. Composition Analysis Method of Mixed Pigment

The K/S of n basic pigments are SP_1, SP_2,…, SP_n, where $SP_i=[SP_{i1}, SP_{i2}.....SP_{iT}]$, $i=1,2.....n$. The K/S of m mixed pigments are DP_1, DP_2,…, DP_m, where $DP_j=[DP_{j1}, DP_{j2}.....DP_{jT}]$ and $j=1,2.....m$. The mixing process is expressed as $DP_p=\sum_{q=1}^{n} c_{pq} * SP_q$, where c_{pq} is the mixing coefficient, $p=1,2.....m$, $q=1,2.....n$, and "*" represents vector-scalar multiplication. With vector representation, $SP=[SP_1, SP_2....SP_n]^T$, $DP=[DP_1, DP_2.....DP_m]^T$ and $C=\lfloor c_{pq} \rfloor_{m\times n}$, the above mixing process can be written $DP=C*SP$.

If K/S of basic pigment and mixed pigment meet the separable condition of mixed signal, DP of mixed pigment can be proceed by FastICA algorithm. The output is $\overline{SP}=[\overline{SP}_1, \overline{SP}_2 ..... \overline{SP}_n]^T$, where $\overline{SP}$ is an approximate representation of SP. The types of n basic pigments corresponding to $\overline{SP}$ are determined by calculating the spectrum similarities between $\overline{SP}$ and all known pigments. The reflection spectrums of n basic pigments are SP_1', SP_2',…, SP_n'. The vector representation is $SP'=[SP_1', SP_2'.....SP_n']^T$, where SP' is an accurate representation of SP. That is to say $DP=C'*SP'$. Thus, the mixing matrix is $C'=DP*(SP')^{-1}$.

One thing to note here is that K/S of actual basic pigments may exist correlation, although the one in our experiment are independent each other. Therefore, the actual data must be de decorrelated. The main decorrelation methods include Karhunen-Loeve Transform (KLT) [23], decorrelation-stretch Transform [24], wavelet transform [25], etc. Sometimes, orthogonalization is required, and the main methods include gram-schmidt transform [26], householder transformation [27], etc.

3.2. Effect Evaluation

First of all, SP and SP' are normalized. After that, the effect evaluation is carried out with the following methods. In these formulas, i and j are serial number of pigments, their ranges are $i=1,2.....n$ and $i=1,2.....n$, SP_{it} is the actual data, and SP_{it}' is the separated result.

(1) Relative mean square error (RMSE)

The RMSE of i-th pigment is shown in formula 15.

$$RMSE_i=\frac{1}{T}\sum_{t=1}^{T}\left[\frac{SP_{it}-SP_{it}'}{SP_{it}}\right]^2 \qquad (15)$$

(2) Signal to Noise Ratio (SNR)

Let SP_i is signal, and $SP_i'-SP_i$ is noise. Then, the SNR of i-th pigment is shown in formula 16.

$$SNR_i=10log_{10}\left(\frac{\sum_{t=1}^{T}(SP_{it})^2}{\sum_{t=1}^{T}(SP_{it}'-SP_{it})^2}\right) \qquad (16)$$

(3) Similarity

The similarity between SP_i and SP_j' is shown in formula 17.

$$\xi_{ij}=\xi(SP_i, SP_j')=\frac{\left|\sum_{t=1}^{T} SP_{it}SP_{jt}'\right|}{\sqrt{\sum_{t=1}^{T} SP_{it}^2 \sum_{t=1}^{T}(SP_{jt}')^2}} \qquad (17)$$

4. EXPERIMENTS AND RESULTS

4.1. Material

Munsell color system is proposed by American chromatist Munsell. And it has become one of the recognized color systems after repeated revisions by American National Standards Institute (ANSI) and Optical Society of America (OSA). For this method, three elements (hue, brightness and saturation) of all sorts of color can be described with the Munsell color cube as shown in figure 5.

Journal of Theoretical and Applied Information Technology
20th June 2014. Vol. 64 No.2

ISSN: 1992-8645 www.jatit.org E-ISSN: 1817-3195

Figure 5: Munsell color cube

According to brightness and reflectivity, Munsell color system is divided into two kinds: full gloss and semi-gloss. The full gloss that includes 1600 spectrums of Munsell color card was chosen in our experiment. The reflection spectrum database was constructed by downloading the full gloss spectral curves from Website of Spectral Color Research group (http://www.uef.fi/fi/spectral/home). The simulated spectrum was generated by mixing spectrum of this database. And the experiments of composition analysis of mixed pigment were carried out under the circumstance of normality and disturbance.

4.2. Composition Analysis Experiment under Normal

The K/S curves of four chosen Munsell color cards are shown in figure 6. In every subfigure, x-coordinate represents wavelength whose range is from 400nm to 780nm, and y-coordinate is K/S. The subfigure's name is the color numbers in Munsell color system. For convenience of description, these curves are called original K/S curves.

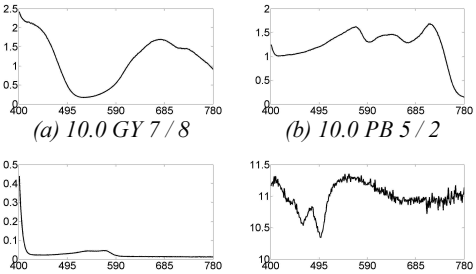

(a) 10.0 GY 7 / 8 *(b) 10.0 PB 5 / 2*

(c) 10.0 PP 9 / 2 *(d) Neutral 0.75*

Figure 6: Original K/S curves

Three groups of mixed K/S curves were generated by multiplying original K/S curves and mixing matrixes M_1, M_2 and M_3, as shown in figure 7. They are called group 1, group 2 and group 3. The number of K/S curves in each group is 4 ,5 and 6. These curves are called mixed K/S curves.

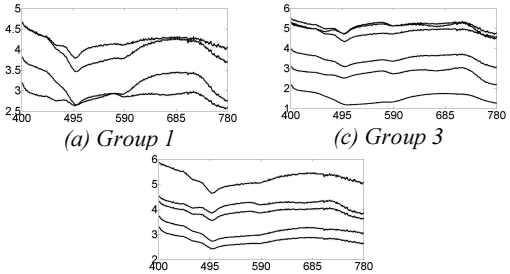

(a) Group 1 *(c) Group 3*

(b) Group 2

Figure 7: Mixed K/S curves

$$M_1 = \begin{bmatrix} 0.23 & 0.10 & 0.48 & 0.46 \\ 0.10 & 0.23 & 0.29 & 0.20 \\ 0.33 & 0.45 & 0.03 & 0.05 \\ 0.34 & 0.22 & 0.20 & 0.29 \end{bmatrix} \quad (18)$$

$$M_2 = \begin{bmatrix} 0.15 & 0.42 & 0.31 & 0.20 & 0.25 \\ 0.30 & 0.10 & 0.01 & 0.22 & 0.05 \\ 0.22 & 0.06 & 0.43 & 0.27 & 0.48 \\ 0.33 & 0.42 & 0.25 & 0.31 & 0.22 \end{bmatrix} \quad (19)$$

$$M_3 = \begin{bmatrix} 0.38 & 0.07 & 0.29 & 0.30 & 0.18 & 0.19 \\ 0.17 & 0.51 & 0.17 & 0.33 & 0.51 & 0.33 \\ 0.37 & 0.03 & 0.15 & 0.12 & 0.14 & 0.07 \\ 0.08 & 0.39 & 0.39 & 0.25 & 0.17 & 0.41 \end{bmatrix} \quad (20)$$

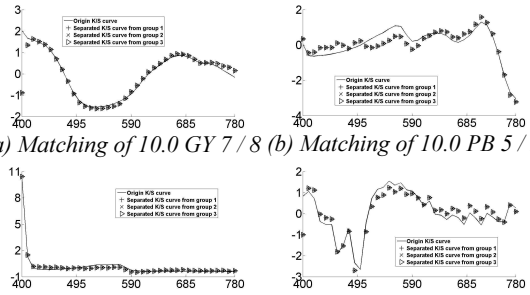

(a) Matching of 10.0 GY 7 / 8 *(b) Matching of 10.0 PB 5 / 2*

(c) Matching of 10.0 PP 9 / 2 *(d) Matching of Neutral 0.75*

Figure 8: Matching between original K/S curves and separated K/S curves

Three groups of mixed K/S curves were processed with FastICA algorithm. The number of decomposed K/S curves in each group is four. These curves are called separated K/S curves. The correspondence between separated K/S curves and original K/S curves was determined by comparing spectrum similarities between them. In order to improve the matching effect, all original K/S curves and separated K/S curves were normalized. The matching result is shown in figure 8. In every subfigure, original K/S curves are shown with

Journal of Theoretical and Applied Information Technology
20th June 2014. Vol. 64 No.2

ISSN: 1992-8645 www.jatit.org E-ISSN: 1817-3195

solid line, and three corresponding separated K/S curves are shown with scatter diagrams that are consisted by cross, "X" mark and right-pointing triangle respectively.

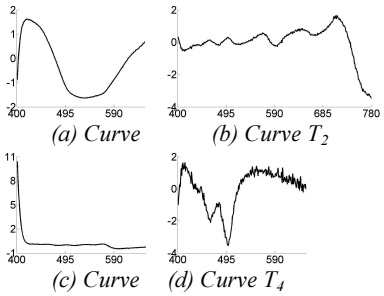

(a) Curve *(b) Curve T_2* *(c) Curve* *(d) Curve T_4*

Figure 9: Average separated K/S

In order to facilitate evaluation, the separated K/S curves of figure 8 were averaged. In figure 9, curves T_1, T_2, T_3 and T_4 are average separated K/S curves of figure 8.a, 8.b, 8.c and 8.d, and they are corresponding to figure 6.a, 6.b, 6.c and 6.d respectively. According to criterions in section 3.2, SP_{it} and $SP_{it}^{'}$ were generated from curve data of figure 6 and figure 9, and RMSE, SNR and similarity were calculated, as shown in table 1. In this table, all RMSE are less than 10^{-5}. It indicates that the separated K/S curve of this method is close to the actual one.

Table 1: Effect evaluation of separated K/S curves

Criterion / Separated K/S curve	RMSE	SNR	Similarity
Curve T_1	0.00000433	10.9028	0.9594
Curve T_2	0.00000955	9.1851	0.9397
Curve T_3	0.00000069	14.8806	0.9837
Curve T_4	0.00000633	10.0796	0.9509

The percentage of basic pigment in each group was calculated. According to method in section 3.1, DP of group 1, 2 and 3 were generated from curve data of figure 7.a, 7.b and 7.c, $SP^{'}$ was generated from curve data of original K/S curves in figure 8, and percentage was calculated with $C^{'} = DP * \left(SP^{'}\right)^{-1}$, as shown in table 2. In this table, the calculated percentage is similar with formula 18, 19 and 20. The results demonstrate that this method can get accurate percentage.

4.3. Composition Analysis Experiment under Disturb

In order to test the anti-interference performance of this method, each group of mixed K/S curves was mixed with one different K/S curve, and they are called new mixed K/S curves. In figure 10, curves R_1, R_2 and R_3 were added into group 1, 2 and 3 respectively. These additional K/S curves are called original disturbance K/S curves.

Mixed K/S curve / Original K/S curve	Group 1					
	Curve1	Curve2	Curve3	Curve4		
10.0 GY 7 / 8	0.23	0.10	0.49	0.46		
10.0 PB 5 / 2	0.10	0.23	0.29	0.20		
10.0 PP 9 / 2	0.33	0.45	0.02	0.04		
Neutral 0.75	0.34	0.22	0.20	0.30		
Mixed K/S curve / Original K/S curve	Group 2					
	Curve1	Curve2	Curve3	Curve4	Curve5	
10.0 GY 7 / 8	0.15	0.42	0.31	0.19	0.24	
10.0 PB 5 / 2	0.30	0.10	0.01	0.22	0.06	
10.0 PP 9 / 2	0.22	0.06	0.43	0.28	0.48	
Neutral 0.75	0.33	0.42	0.25	0.31	0.22	
Mixed K/S curve / Original K/S curve	Group 3					
	Curve1	Curve2	Curve3	Curve4	Curve5	Curve6
10.0 GY 7 / 8	0.38	0.08	0.29	0.30	0.17	0.19
10.0 PB 5 / 2	0.17	0.50	0.17	0.34	0.51	0.33
10.0 PP 9 / 2	0.37	0.03	0.15	0.12	0.14	0.07
Neutral 0.75	0.08	0.39	0.39	0.24	0.18	0.41

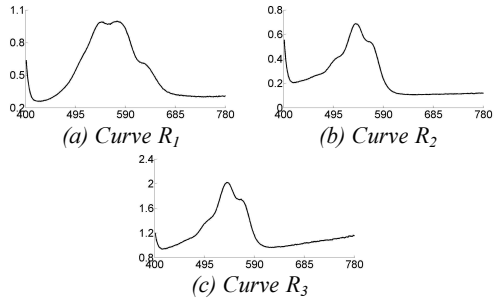

(a) Curve R_1 *(b) Curve R_2* *(c) Curve R_3*

Figure 10: Original disturbance K/S curves

Table 2: Calculated percentage of each group

The new mixed K/S curves were processed with FastICA algorithm, and the number of decomposed K/S curves in each group is five. The five K/S curves in each group can be divided into two kinds by comparing similarities between them and original K/S curves. One is four separated original K/S curves that correspond to the original K/S curves of figure 6. The other is one separated disturbance K/S curve that corresponds to the disturbance K/S curve of figure 10.

In the following, the five mixed K/S curves by adding disturbance K/S curve R_1 into mixed K/S curves of figure 7.a is taken as an example for describing the classification method. The five

ISSN: 1992-8645 www.jatit.

separated K/S curves of FastICA algorithm are shown in figure 11, and the similarity matrix between them and original K/S curves is shown in table 3. In this table, the maximum absolute values of similarity in row 1, 2, 3 and 4 are more than 0.929, but the one in row 5 is less than 0.24. Thus, it can conclude that curves F_1, F_2, F_3 and F_4 are separated original K/S curves, and curve F_5 is a separated disturbance K/S curve.

Table 3: Similarity and correspondence between the separated K/S curve and the original K/S curve

Original *K/S* curve / Separated *K/S* curve	10.0 GY 7 / 8	10.0 PB 5 / 2	10.0 PP 9 / 2	Neutral 0.75	Correspondence
Curve F_1	0.2753	-0.0326	**0.9825**	0.1505	10.0 PP 9 / 2
Curve F_2	0.0376	**0.9307**	0.0266	-0.0738	10.0 PB 5 / 2
Curve F_3	**0.9294**	-0.1952	-0.1745	-0.2383	10.0 GY 7 / 8
Curve F_4	-0.0520	0.2294	0.0599	**0.9524**	Neutral 0.75
Curve F_5	0.2374	-0.2049	0.0054	0.0893	disturbance

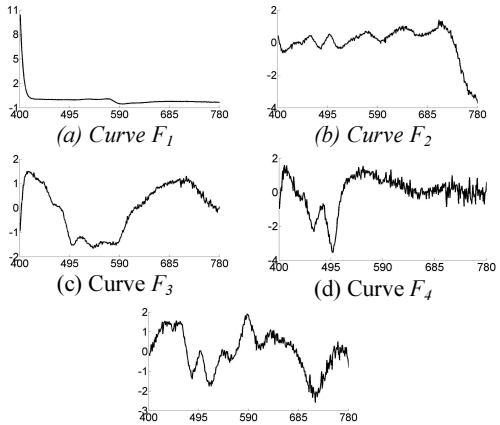

(a) Curve F_1 *(b) Curve F_2* *(c) Curve F_3* *(d) Curve F_4* *(e) Curve F_5*

Figure 11: Separated K/S curves of FastICA

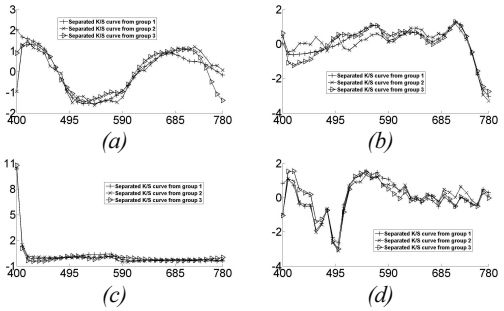

(a) *(b)* *(c)* *(d)*

Figure 12: Separated original K/S curves under the circumstance of disturbance

According to the above steps, the separated K/S curves of other groups were generated, as shown in figure 12 and 13. The separated original K/S curves corresponding to figure 6.a, 6.b, 6.c and 6.d are shown in figure 12.a, 12.b, 12.c and 12.d, and

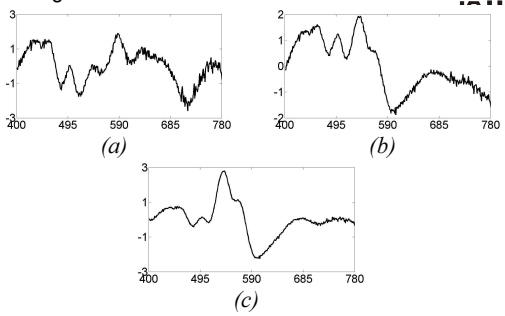

(a) *(b)* *(c)*

Figure 13: Separated disturbance K/S curves under the circumstance of disturbance

each subfigure have three K/S curves derived from three groups. The separated disturbance K/S curves corresponding to figure 10.a, 10.b and 10.c are shown in figure 13.

The separated original K/S curves in figure 12 were averaged, as shown in figure 14. In this figure, curves G_1, G_2, G_3 and G_4 correspond to figure 6.a, 6.b, 6.c and 6.d. According to this correspondence and the criterions in section 3.2, the evaluation results were calculated, as shown in table 4. In this table, all RMSE are less than 10^{-5}. The results show the robust of this method under disturbance.

Table 4: Effect evaluation of separated original K/S curves

Criterion / Separated *K/S* curve	RMSE	SNR	Similarity
Curve G_1	0.00000360	11.3021	0.9630
Curve G_2	0.00000152	13.1710	0.9759
Curve G_3	0.00000079	14.6047	0.9827
Curve G_4	0.00000725	9.7845	0.9475

Before calculating percentage, the original disturbance K/S curve must be deleted from the new mixed K/S curves. For each separated disturbance K/S curves of figure 13, the spectrum similarities between it and original disturbance K/S curves of figure 10 are more than the one between them and mixed K/S curves of figure 7. Therefore, the new mixed K/S curve with the largest spectrum similarity is the original disturbance K/S curve. After deleting original disturbance K/S curves, the mixed K/S curves of figure 7 are restored, and the percentage was calculated according to the method in section 3.1, as shown in table 5. The result of this table is similar with formula 18, 19 and 20. These data demonstrate that this method can get accurate percentage.

ISSN: 1992-8645 www.jatit.org E-ISSN: 1817-3195

Table 5: Calculated percentage of each group

Mixed K/S curve / Original K/S curve	Group1					
	Curve1	Curve2	Curve3	Curve4		
10.0 GY 7 / 8	0.23	0.10	0.48	0.46		
10.0 PB 5 / 2	0.10	0.24	0.29	0.21		
10.0 PP 9 / 2	0.33	0.45	0.03	0.05		
Neutral 0.75	0.34	0.21	0.20	0.28		
Mixed K/S curve / Original K/S curve	Group2					
	Curve1	Curve2	Curve3	Curve4	Curve5	
10.0 GY 7 / 8	0.15	0.42	0.31	0.20	0.25	
10.0 PB 5 / 2	0.31	0.10	0.01	0.22	0.05	
10.0 PP 9 / 2	0.21	0.06	0.43	0.28	0.48	
Neutral 0.75	0.33	0.42	0.25	0.30	0.22	
Mixed K/S curve / Original K/S curve	Group3					
	Curve1	Curve2	Curve3	Curve4	Curve5	Curve6
10.0 GY 7 / 8	0.38	0.07	0.29	0.30	0.18	0.19
10.0 PB 5 / 2	0.17	0.50	0.17	0.33	0.52	0.33
10.0 PP 9 / 2	0.37	0.03	0.15	0.12	0.14	0.07
Neutral 0.75	0.08	0.40	0.39	0.25	0.16	0.41

5. CONCLUSION

The composition analysis of mixed pigment has extensive application space. RS is a commonly used method in this field, but the accuracy of type judgment of basic pigment would be affected to some extent. In our study, the mixed pigments are expressed as spectrums, and the types and percentages of basic pigments are determined by integrating with ICA, spectrum similarity, Kubelka-Munk theory, etc. To validate this method, the experiment with simulated spectrum from Munsell color system was carried out. The results demonstrate that the type and percentage of basic pigment can be determined accurately under the circumstance of normality and disturbance, which meets the traceability of mixed pigment.

In this paper, the composition analysis method of mixed pigment based on spectrum expression and ICA is proposed and proved, but it is only the beginning. In practice, a lot of elements should be considered. In order to improve its practicability, decorrelation and orthogonalization would be integrated with our study.

ACKNOWLEDGMENT

The authors are grateful to Yingqing Xu for his discussion and suggestion about background knowledge, validity, experiment, etc. This work was supported by National Basic Research Program of China (Grant No. 2012CB725300), National Natural Science Foundation of China (Grant No. 61373072) and China Postdoctoral Science Foundation (Grant No. 2013M530035).

REFRENCES:

[1] J. D. Wilson, G. M. LaPorte, and A. A. Cantu. "Differentiation of black gel ink using optical and chemical techniques", *Journal of Forensic Sciences*, Vol. 49, No. 2, 2004, pp. 364-370.

[2] W. S. Han, and L. Q. Wang. "Application of spectral technologies in analyzing pigments of colored relics", *Spectroscopy and Spectral Analysis*, Vol. 32, No. 12, 2012, pp. 3394-3398.

[3] Y. L. Pan, B. S. Zhang, and Q. Xu. "Research on application of principal component analysis in computer color matching for textile dyeing", *Journal of Qingdao University(Engineering & Technology)*, Vol. 26, No. 4, 2011, pp. 19-22,28.

[4] G. Dupuis, M. Elias, and L. Simonot. "Pigment Identification by Fiber-Optics Diffuse Reflectance Spectroscopy", *Applied Spectroscopy*, Vol. 56, No. 10, 2002, pp. 1329-1336.

[5] G. P. Petropoulos, K. P. Vadrevu, G. Xanthopoulos, G. Karantounias, M. Scholze. "A Comparison of Spectral Angle Mapper and Artificial Neural Network Classifiers Combined with Landsat TM Imagery Analysis for Obtaining Burnt Area Mapping", *Sensors*, Vol. 10, No. 3, 2010, pp. 1967-1985.

[6] S. P. Zhang. "Based on the multispectral imaging of research on method of the color rejuvenation of Chinese paintings", *Master thesis of Tianjin University*, Tianjin, China, 2010, pp. 8-10.

[7] R. E. Bellman, R. Corporation. "Dynamic programming", Princeton University Press (America), 1957, pp. 304-315.

[8] K. Beyel, J. Goldstein, R. Ranmakrishnan. "When Is 'Nearest Neighbor' Meaningful", *Proceedings of the International Conference on Database Theory*, Springer-Verlag Press (Germ any) , 1999, pp. 217-235.

[9] A. Hyvärinen, J. Karhunen, E. Oja. "Independent Component Analysis", Wiley-Interscience (America), 2001, pp. 23-47.

[10] H. Grassmann. "Zur Theorie der Farbenmischung", *Annalen der Physik*, Vol. 165, No. 5, 1853, pp. 69-84.

ISSN: 1992-8645 www.jatit.org E-ISSN: 1817-3195

[11] N. Moroney, M. D. Fairchild, R. W. Hunt. "The CIECAM02 color appearance model", *Proceedings of IS&T/SID 10th Color Imaging Conference*, Curran Associates. Inc (Ireland), 2002, pp. 33-38.

[12] T. Smith, J. Guild. "The CIE colorimetric standards and their use", *Transactions of the Optical Society*, Vol. 33, No. 3, 1931, pp. 73-134.

[13] B. Sun, W. P. Yang, D. D. Hou, etc. "Designing study of multi-spectral imaging system based on two CMOS", *Journal of Yunnan Normal University*, Vol. 28, No. 2, 2008, pp. 32-36.

[14] R. S. Berns. "Billmeyer and Saltzman's Principles of Color Technology", Translated by X. M. LI, R. Ma, L. R. Chen, Chemical Industry Press (China), 2002, pp. 34-37.

[15] P. Kubelka, F. Munk. "Ein Beitrage zur Optik der Farbanstriche", *Zeitschrift fur technische Physik*, Vol. 12, No. 11, 1931, pp. 593-601.

[16] M. S. Pedersen, J. Larsen, U. Kjems, L. C. Parra Dr. "Convolutive Blind Source Separation Methods", Springer Handbook of Speech Processing, Springer-Verlag Press (Germ any), 2008, pp. 1065-1094.

[17] E. Hoffmann, D.Kolossa, R. Orglmeister. "A Batch Algorithm for Blind Source Separation of Acoustic Signals Using ICA and Time-Frequency Masking", *Lecture Notes in Computer Science*, Vol. 4666, 2007, pp. 480-487.

[18] W. H. Fu, X. N. Yang, N. A. Liu, X. W. Zeng. "Blind source separation algorithm for communication complex signals in communication reconnaissance", *Frontiers of Electrical and Electronic Engineering in China,* Vol. 3, No. 3, 2008, pp. 338-342.

[19] K. R. Muller, R. Vigario, F. Meinecke, A. Ziehe. "Blind Source Separation Techniques for Decomposing Event-Related Brain Signals", *International Journal of Bifurcation and Chaos*, Vol. 14, No. 2, 2004, pp. 773-791.

[20] K. H. Liu, W. H. Dragoset. "Blind-source separation of seismic signals based on information maximization", *Geophysics*, Vol. 78, No. 4, 2012, pp. 119-130.

[21] A. Kumar, S. S. Ghose, M. K. Ghose. "An Improved Secure Data Communication Using Blind Source Separation and Chaos", *Proceedings of ISM '09. 11th IEEE International Symposium on Multimedia*, IEEE Computer Society (America), 2009, pp. 358-362.

[22] G. B. Li, J. Y. Zhang, Y. X. Mao. "The development and research status of blind source separation", *Aerospace Electronic Warfare*, Vol. 23, No. 6, 2004, pp. 13-16,23.

[23] R. J. Mathar. "Karhunen–Loeve basis functions of Kolmogorov turbulence in the sphere", *Baltic Astronomy*, Vol. 13, No. 3,4, 2008, pp. 383-398.

[24] A. R. Gillespie, A. B. Kahle, R. E. Walker. "Color enhancement of highly correlated images. I. Decorrelation and HSI contrast stretches", *Remote Sensing of Environment*, Vol. 20, No. 3, 1986, pp. 209-235.

[25] B. K. Alsberg, A. M. Woodward, D. B. Kell. "An introduction to wavelet transforms for chemometricians: A time-frequency approach", *Chemometrics and Intelligent Laboratory Systems*, Vol. 37, No. 2, 1997, pp. 215-239.

[26] J. R. Rice. "Experiments on Gram-Schmidt orthogonalization", *Mathematics of Computation*, Vol. 20, No. 94, 1966, pp. 325-328.

[27] A. S. Householder. "Unitary Triangularization of a Nonsymmetric Matrix", *Journal of the ACM*, Vol. 5, No. 4, 1958, pp. 339-342.